Protein Backbone Dynamics Revealed by Quasi Spectral Density Function Analysis of Amide N-15 Nuclei

Rieko Ishima* and Kuniaki Nagayama

Nagayama Protein Array Project, ERATO, JRDC, Tsukuba Research Consortium, Pilot Laboratory, 5-9-1 Tokodai, Tsukuba, 300-26 Japan, and Department of Pure and Applied Sciences, College of Arts and Sciences, The University of Tokyo, Komaba, Meguro, Tokyo, 153 Japan

Received August 16, 1994; Revised Manuscript Received December 13, 1994[⊗]

ABSTRACT: Spectral density functions $J(0)$, $J(\omega_N)$, and $J(\omega_H + \omega_N)$ of individual amide N-15 nuclei in proteins were approximated by a quasi spectral density function (QSDF). Using this function, the backbone dynamics were analyzed for seven protein systems on which data have been published. We defined $J(0; \omega_N)$ as the difference between the $J(0)$ and the $J(\omega_N)$ values, which describes motions slower than 50 (or 60) MHz, and $J(\omega_N; \omega_{H+N})$ as the difference between the $J(\omega_N)$ and the $J(\omega_H + \omega_N)$ values, which describes motions slower than 450 (or 540) MHz. The QSDF analysis can easily extract the $J(0; \omega_N)$ of protein backbones, which have often some relation to biologically relevant reactions. Flexible N-terminal regions in eglin *c* and glucose permease IIA and a loop region in eglin *c* showed smaller values of both the $J(0; \omega_N)$ and the $J(\omega_N; \omega_{H+N})$ as compared with the other regions, indicating increases in motions faster than nanosecond. The values of the $J(0; \omega_N)$ for the backbone of the FK506 binding protein showed a large variation in the apoprotein but fell in a very narrow range after the binding of FK506. Characteristic increase or decrease in the values of $J(0)$ and $J(\omega_N)$ was observed in two or three residues located between secondary structures.

Precise measurements of the C-13 and N-15 relaxation of individual nuclei in proteins in solution are possible (Nirmala & Wagner, 1988; Wagner, 1993) due to developments in heteronuclear detection used in NMR[1] and stable isotope labeling techniques (Bax et al., 1983; Griffey et al., 1985; Peng et al., 1991; Kay et al., 1992). The relaxation times of C-13 and N-15 nuclei contain information on internal motions represented by angular fluctuations of each C−H vector or N−H vector, respectively. These relaxation times contrast with the relaxation of protons, where magnetization is rapidly equilibrated among neighboring protons by cross relaxation (Ishima et al., 1991). Amide N-15 is used as a probe to evaluate backbone dynamics of proteins due to its low resonance frequency compared with that of protons.

Currently, there are two methods used to analyze N-15 relaxation data. One is the model-free analysis (Lipari & Szabo, 1982a,b), and the other is the mapping of the spectral densities (Peng & Wagner, 1992a,b). The model-free analysis is widely accepted in evaluating fast internal motions by combining a generalized order parameter (S^2) and one or two effective correlation times (τ_e; Clore et al., 1990). As Peng and Wagner (1992a) pointed out, however, the physical meaning of the τ_e is not yet well explained. A merit of the model-free analysis is its simple treatment of using only one set of three relaxation times for each N-15 nucleus. Peng and Wagner (1992b) introduced a very interesting analysis by mapping spectral densities. In this analysis, the relaxation times are replaced by the spectral densities, which reflect the frequency components in the molecular motional process coupled with internal motions and the molecular tumbling. To overcome the tedious job of obtaining six relaxation times inherent in this method, we introduced a simplified method, the quasi spectral density function (QSDF) analysis (Ishima & Nagayama, 1995). It needs only three relaxation times: longitudinal relaxation time (T_1), a transverse relaxation time (T_2), and heteronuclear cross-relaxation time (RN^{-1}). These three relaxation times derive the spectral densities, $J(0)$, $J(\omega_N)$, and $J(\omega_H + \omega_N)$, where ω_N and ω_H are the angular frequencies of protons and nitrogen, respectively.

Our approach in using the QSDF analysis emphasizes extracting the spectral densities as primary information on protein dynamics and then interpreting these spectral densities with proper motional models. In this paper, first we describe the QSDF method and characterize the spectral densities of $J(0)$, $J(\omega_N)$, and $J(\omega_H + \omega_N)$ in terms of internal dynamics and overall rotation of protein molecules. Then we show results of the QSDF analysis for five proteins, on which N-15 relaxation data have been published (Cheng et al., 1993, 1994; Peng & Wagner, 1992a; Kraulis et al., 1994; Stone et al., 1992, 1993). Finally, we discuss the new insights into protein dynamics provided by the QSDF analysis.

THEORETICAL

The QSDF Analysis. Explicit expressions of N-15 relaxation times have been given (Goldman, 1984; Kay et al., 1992), where the dipolar interaction with attached protons and the chemical shift anisotropy of N-15 nuclei have been taken into account in the relaxation mechanisms. In these expressions, the spectral densities with five angular frequencies are used to obtain T_1, T_2, and RN.

* To whom correspondence should be addressed at the Tsukuba Research Consortium.

[⊗] Abstract published in *Advance ACS Abstracts,* February 1, 1995.

[1] Abbreviations: NMR, nuclear magnetic resonance; QSDF analysis, quasi spectral density function analysis; T_1, longitudinal relaxation time; T_2, transverse relaxation time; RN, heteronuclear cross-relaxation rate; NOE, nuclear Overhauser effect.

0006-2960/95/0434-3162$09.00/0

$$T_1^{-1} = (1/4)D_{NH}[J(\omega_H - \omega_N) + 3J(\omega_N) + 6J(\omega_H + \omega_N)] + (1/3)C_{SA}[J(\omega_N)] \quad (1)$$

$$T_2^{-1} = (1/8)D_{NH}[4J(0) + 3J(\omega_N) + J(\omega_H + \omega_N) + 6J(\omega_H) + 6J(\omega_H + \omega_N)] + (1/18)C_{SA}[4J(0) + 3J(\omega_N)] \quad (2)$$

$$RN = (1/4)D_{NH}[6J(\omega_H + \omega_N) - J(\omega_H - \omega_N)] \quad (3)$$

The RN is derived from NOE by the relationship

$$NOE = 1 + \gamma_H/\gamma_N RNT_1 \quad (4)$$

where D_{NH} and C_{SA} are constants given by $\gamma_H^2\gamma_N^2\hbar^2/r^6$ and $\Delta^2\omega_N^2$, respectively, in which γ_H and γ_N are the gyromagnetic ratios of proton and nitrogen, respectively, $\hbar$ is the Boltzman constant divided by 2π, r is the distance between proton and nitrogen, and Δ is the chemical shift anisotropy of the nitrogen.

It needs the other relaxation times in addition to the above three (Peng & Wagner, 1992b) in order to determine the spectral densities because the spectral densities at five different frequencies already take part in eqs 1−3. In order to determine spectral densities only from the set of three relaxation times, we have to decrease the number of independent arguments in eqs 1−3. Equation 5 is proposed in the QSDF analysis.

$$J(\omega_H + \omega_N) \simeq J(\omega_H) \simeq J(\omega_H - \omega_N) \quad (5)$$

Thus, eqs 1−3 simplify to

$$T^{-1} = (1/4)D_{NH}[3J(\omega_N) + 7J(\omega_H + \omega_N)] + (1/3)C_{SA}[J(\omega_N)] \quad (6)$$

$$T^{-2} = (1/8)D_{NH}[4J(0) + 3J(\omega_N) + 13J(\omega_H + \omega_N)] + (1/18)C_{SA}[4J(0) + 3J(\omega_N)] \quad (7)$$

$$RN = (1/4)D_{NH}[5J(\omega_H + \omega_N)] \quad (8)$$

Now, the three relaxation rates T_1^{-1}, T_2^{-1}, and RN are sufficient to determine the three spectral densities, namely, $J(0)$, $J(\omega_N)$, and $J(\omega_H + \omega_N)$.

Equation 5 is validated in the case of the monotonically decreasing function of $J(\omega_i)$ around $\omega_H \pm \omega_N$ (Ishima & Nagayama, 1995). The angular frequencies of $\omega_H + \omega_N$, ω_H, and $\omega_H - \omega_N$ are very close to each other comparing with the angular frequency of ω_N, and hence, the small differences in the corresponding spectral density values can be ignored. Since the sign of the gyromagnetic ratio of N-15 is opposite to that of the proton, the $J(\omega_H + \omega_N)$ is slightly larger than the $J(\omega_H - \omega_N)$. Therefore, eq 8 was derived. In this paper, monotonically decreasing the spectral density function is assumed around $\omega_H \pm \omega_N$.

Significance of the Spectral Densities J(0), J(ω_N), and J(ω_H + ω_N). The motional process with correlation times close to the inverse of ω_i mainly contributes to the spectral density value of $J(\omega_i)$. The $J(\omega_i)$ results from the Fourier transform of the correlation function $C(\tau)$ of an interaction vector (Slicter, 1978).

$$J(\omega_i) = 2\int_0^\infty C(\tau)\cos\omega_i\tau\, d\tau \quad (9)$$

The $C(\tau)$ is obtained by the back-transform of the $J(\omega_i)$:

$$C(\tau) = 1/\pi\int_{-\infty}^{\infty} J(\omega_i)\exp(i\omega_i\tau)\, d\omega \quad (10)$$

Equation 9 indicates that the value of $J(0)$ is the summation of the autocorrelation over time. Any motion can contribute to the $J(0)$. Equation 10 indicates that the $C(0)$, which is the correlation without lag, is the summation of all $J(\omega_i)$ values over the angular frequency ω_i. Integration of the $J(\omega_i)$ over frequency is a constant. Only the distribution of the $J(\omega_i)$ values are changed against ω_i. An increase in the $J(\omega_i)$ at a frequency should be compensated by a decrease in the $J(\omega_i)$ at another frequency. This trend in the $J(\omega_i)$ is independent of the combination of internal motions.

As mentioned, we expect that the values of $J(\omega_N)$ and $J(\omega_H + \omega_N)$ mainly reflect nano- and picosecond motions. It is, however, necessary to clarify the motion represented in the $J(\omega_i)$ quantitatively. First, we consider a general expression of the $J(\omega_i)$ function for an interaction vector perturbed with various motional processes. Due to the overall isotropic rotation of proteins, each random motional process can be safely decomposed into a sum of exponential decays reflected in the autocorrelation function (Fujiwara & Nagayama, 1985). The final autocorrelation function is then described by a sum of an enormous number of exponential decays, which finally lead to the well-known form of the spectral density (King & Jardetzky, 1978; Ribeiro et al., 1980).

$$J(\omega_j) = (2/5)\sum_i^{\xi} \frac{a_i\tau_i}{1 + \tau_i^2\omega_j^2} \quad (11)$$

Individual relaxation components are characterized by amplitudes a_i and effective correlation times, the τ_i including the contribution from the overall rotation.

$$\sum_i^{\xi} a_i = 1 \quad (12)$$

$$\tau_1 > \tau_2 > \tau_3 > \tau_4 > \ldots > \tau_\xi \quad (13)$$

When the overall rotation and internal motions are mutually independent, τ_i is expressed as

$$\tau_i = (\tau_i'^{-1} + \tau_R^{-1})^{-1} \quad (14)$$

where τ_i is the correlation time of the ith exponential and the τ_R is that of the overall rotation of the molecule. We note here that the ith term in eq 11 does not necessarily correspond to the individual ith motional process (Lipari & Szabo, 1982a; Fujiwara & Nagayama, 1985). Using eq 11, the spectral densities of $J(0)$, $J(\omega_N)$, and $J(\omega_H + \omega_N)$ are described as

$$J(0) = (2/5)[a_1\tau_1 + a_2\tau_2 + \ldots + a_\xi\tau_\xi] \quad (15)$$

$$J(\omega_N) = (2/5)\left[\frac{a_1\tau_1}{1 + \tau_1^2\omega_N^2} + \frac{a_2\tau_2}{1 + \tau_2^2\omega_N^2} + \ldots + \frac{a_{N+p}\tau_{N+p}}{1 + \tau_{N+p}^2\omega_N^2} + a_{N+p+1}\tau_{N+p+1} + a_{N+p+2}\tau_{N+p+2} \ldots + a_\xi\tau_\xi\right] \quad (16)$$

$$J(\omega_H + \omega_N) = (2/5)\left[\frac{a_1\tau_1}{1+\tau_1^2\omega_{H+N}^2} + \frac{a_2\tau_2}{1+\tau_2^2\omega_{H+N}^2} + \right.$$
$$\ldots + \frac{a_N\tau_N}{1+\tau_N^2\omega_{H+N}^2} + \frac{a_{H+N+q}\tau_{H+N+q}}{1+\tau_{H+N+q}^2\omega_{H+N}^2} +$$
$$\left. a_{H+N+q+1}\tau_{H+N+q+1} + a_{H+N+q+2}\tau_{H+N+q+2} \ldots + a_\xi\tau_\xi\right] \quad (17)$$

Here, when $\tau_i^2\omega_j^2 \ll 1$, we can use the approximation given by eq 18. The values of τ_N and τ_{H+N} are ω_N^{-1} and ω_{H+N}^{-1}, respectively. The τ_{N+p} and τ_{H+N+q} are the arbitrary cutoff correlation times in the regions $\tau_i^2\omega_N^2 \ll 1$ and $\tau_i^2\omega_{N+H}^2 \ll 1$.

$$\frac{a_i\tau_i}{1+\tau_i^2\omega_j^2} = a_i\tau_i \quad (18)$$

From eqs 16 and 17, the correlation times around ω_N^{-1} or $(\omega_H + \omega_N)^{-1}$ are known to contribute to the $J(\omega_N)$ or the $J(\omega_H + \omega_N)$ although the degree depends on either τ_i or a_i.

Inspection of eqs 15 and 16 suggests to us a new index, $J(0; \omega_N)$, as a difference value between the $J(0)$ and the $J(\omega_N)$.

$$J(0; \omega_N) = J(0) - J(\omega_N)$$
$$= (2/5)\left[\left(a_1\tau_1 - \frac{a_1\tau_1}{1+\tau_1^2\omega_N^2}\right) + \right.$$
$$\left.\left(a_2\tau_2 - \frac{a_2\tau_2}{1+\tau_2^2\omega_N^2}\right) + \ldots + \left(a_{N+p}\tau_{N+p} - \frac{a_{N+p}\tau_{N+p}}{1+\tau_{N+p}^2\omega_n^2}\right)\right] \quad (19)$$

Equation 19 describes that the $J(0; \omega_N)$ represents all relaxation components with correlation times slower than those components that are not included in the $J(\omega_N)$. The terms with shorter τ_i than ω_N^{-1} are neglected in eq 19. Only relaxation components with correlation times longer than τ_{N+p} contribute to the $J(0; \omega_N)$. With a 500- or a 600-MHz spectrometer, the ω_N^{-1} is 3.0 or 2.6 ns, respectively. Therefore, the $J(0; \omega_N)$ represents relaxation components with correlation times slower than nanosecond.

All individual terms in eq 19 can be approximated by $a_i\tau_i$ except for the terms with τ_i values which satisfy $\tau_i^2\omega_N^2 \approx 1$. For example, when we assume τ_i values given by

$$\tau_i = n\omega_N^{-1} \quad \text{or} \quad \tau_i = \omega_N^{-1}/n \qquad n = 1, 2, 3, \ldots \quad (20)$$

eq 19 can be rewritten as

$$J(0; \omega_N) = (2/5)[a_1\tau_1 + a_2\tau_2 + \ldots + 0.9a_{N-2}\tau_N +$$
$$0.8a_{N-1}\tau_N + 0.5a_N\tau_N + 0.2a_{N+1}\tau_N + 0.1a_{N+2}\tau_N \ldots] \quad (21)$$

The contribution of the $a_i\tau_i$ term to the $J(0; \omega_N)$ remains only by a half at $\tau_i = \omega_N^{-1}$. Increases or decreases in the $J(0; \omega_N)$ depend on the redistribution of the a_i values. Increases in the $J(0; \omega_N)$ occur in two cases: a small increase in a_i at large τ_i or a large increase in a_i at small τ_i. We define both cases as effective increases in the motion slower than ω_N^{-1}.

Similarly to the $J(0; \omega_N)$, a difference value between the $J(\omega_H + \omega_N)$ and the $J(\omega_N)$ is defined as $J(\omega_N; \omega_{H+N})$.

$$J(\omega_N; \omega_{H+N}) = J(\omega_N) - J(\omega_H + \omega_N)$$
$$= (2/5)\sum_i^{H+N+q}\left[\left(\frac{a_i\tau_i}{1+\tau_i^2\omega_N^2} - \frac{a_i\tau_i}{1+\tau_i^2\omega_{H+N}^2}\right)\right] \quad (22)$$

The correlation times longer than the ω_{H+N+p}^{-1} contribute to the $J(\omega_N; \omega_{H+N})$. Individual terms in eq 22 are negligibly smaller than $a_i\tau_i$ when the τ_i values satisfy $\omega_{H+N}^2\tau_i^2 > \omega_N^2\tau_i^2 \gg 1$. Individual terms of eq 22 are nearly $a_i\tau_i$ when the τ_i values satisfy $\omega_{H+N}^2\tau_i^2 \gg 1$ and $\omega_N^2\tau_i^2 \ll 1$. When we assume τ_i values given by

$$\tau_i = n\omega_{H+N}^{-1} \quad \text{or} \quad \tau_i = \omega_{H+N}^{-1}/n \qquad n = 1, 2, 3, \ldots \quad (23)$$

then eq 22 can be rewritten as

$$J(\omega_N; \omega_H + \omega_N) =$$
$$(2/5)\sum_i^{H+N+q}\left[\left(\frac{a_1\tau_1}{1+\tau_1^2\omega_N^2} - \frac{a_1\tau_1}{1+\tau_1^2\omega_{H+N}^2}\right) + \right.$$
$$\left(\frac{a_2\tau_2}{1+\tau_2^2\omega_N^2} - \frac{a_2\tau_2}{1+\tau_2^2\omega_{H+N}^2}\right) + \ldots + a_{N-p}\tau_{N-p} +$$
$$a_{N-p+1}\tau_{N-p+1} + \ldots + a_N\tau_N + a_{N+p}\tau_{N+p} + \ldots +$$
$$0.9a_{H+N-2}\tau_{H+N} + 0.8a_{H+N-1}\tau_{H+N} + 0.5aH_{+N}\tau_{H+N} +$$
$$\left. 0.2a_{H+N+1}\tau_{H+N} + 0.1a_{H+N+2}\tau_{H+N} \ldots\right] \quad (24)$$

where the τ_{N-p} is the cutoff correlation time which satisfies eq 18 at $\omega_j = \omega_N$. Equation 24 indicates that the relaxation components with correlation times longer than the ω_{H+N}^{-1} contribute to the $J(\omega_N; \omega_{H+N})$. The relaxation components with correlation times longer than ω_N^{-1} are not expected to contribute to the $J(\omega_N; \omega_{H+N})$ so much.

In summary, the QSDF method provides a set of the $J(0)$, $J(\omega_N)$, and $J(\omega_H + \omega_N)$ values for individual amide N-15 nuclei in the protein backbone. Because the spectral density function is a distribution of the relaxation components, a spectral density value is a ratio of the fluctuation characterized by a relaxation time to the total fluctuation of the interaction vector. Taking this into account, the spectral density values can be evaluated as follows.

(1) We define two difference functions of the spectral densities: the $J(0; \omega_N)$, which is the difference between the $J(0)$ and the $J(\omega_N)$, and the $J(\omega_N; \omega_{H+N})$, which is the difference between the $J(\omega_N)$ and $J(\omega_{H+N})$. The $J(0; \omega_{H+N})$ and the $J(\omega_N; \omega_{H+N})$ are the sums of the relaxation components that only have correlation times longer than ω_N^{-1} and ω_{H+N}^{-1}, respectively. We denote that the $J(0; \omega_N)$ and the $J(\omega_N; \omega_{H+N})$ describe the motions slower than ω_N^{-1} and ω_{H+N}^{-1}, respectively.

(2) Motions slower than ω_N^{-1} and ω_{H+N}^{-1} are evaluated using the $J(0; \omega_N)$ and the $J(\omega_N; \omega_{H+N})$, since the relaxation

components in the limited ranges contribute to the $J(0; \omega_N)$ and the $J(\omega_N; \omega_{H+N})$ as described in eqs 19 and 22, respectively. Although these ranges may be wider than the effective correlation times actually contributing to the spectral densities, a narrow range of the correlation times always dominates the $J(0; \omega_N)$ and the $J(\omega_N; \omega_{H+N})$, compared with the spectral densities themselves. Another reason for evaluating the $J(0; \omega_N)$ and the $J(\omega_N; \omega_{H+N})$ is that the difference between two spectral densities indicates the slope of the spectral density function between the two frequencies. However, when we are interested in the relative distribution of the spectral density as a whole, such as flatness of the distribution around a particle frequency, it is better to use the ratio of spectral densities at two frequencies (Peng & Wagner, 1992a).

(3) Increases (or decreases) in either a_i or τ_i in eq 19 or 22 can lead to increases (or decreases) in the $J(0; \omega_N)$. We cannot yet separate the contributions of a_i and τ_i. Nevertheless, increases in the $J(0; \omega_N)$ only arise from increases in the relaxation components with correlation times longer than the ω_N^{-1}, namely, the shift of τ_i's for larger values and/or the redistribution of a_i's to weigh the smaller indices corresponding to longer correlation times. We call the increases in the $J(0; \omega_N)$ as increases in the motions slower than ω_N^{-1}. For the same reason, we do not differentiate the exchange term from the motional term in T_2. The former is assumed to be included in $J(0)$ as a low-frequency contribution to the spectral density.

(4) Both internal motions and the overall rotation of the molecule contribute to the $J(0; \omega_N)$, and the $J(\omega_N; \omega_{H+N})$. The exact rotational correlation time of the molecule, therefore, can only be obtained by other technique. However, by comparison of the spectral densities for two states of a protein, changes in the overall rotations can be safely claimed as shown later. This is particularly true for N-15 NMR because the ω_N^{-1} is on the order of nanoseconds, which is on the same order as the rotational correlation times of protein molecules.

PROTEINS

The QSDF analysis was applied to five proteins of which relaxation data had been published: eglin *c* (Peng & Wagner, 1992a), FK506 binding protein (Cheng et al., 1993, 1994), ras p21-GDP (Kraulis et al., 1994), thioredoxin (Stone et al., 1993), and glucose permease IIA domain (Stone et al., 1992). Two states of the proteins were examined for FK506 binding protein and thioredoxin in each. The $J(0)$, $J(\omega_N)$, and $J(\omega_H + \omega_N)$ values were analytically calculated by solving eqs 6−8 on the basis of relaxation data taken from the literature. In most literature, uncertainty of relaxation data or fitting error to relaxation times have been given, which were used to estimate intrinsic errors in the calculation. Six hundred megahertz proton frequency for ras p21 protein and 500 MHz for others were used.

RESULTS AND DISCUSSION

The QSDF Analysis of Eglin c. The $J(0)$, $J(\omega_N)$, and $J(\omega_H + \omega_N)$ values for backbone amide N-15 of eglin *c* are shown in Figure 1. Intrinsic errors of these $J(\omega)$ values were estimated to be 2.2%, 2.0%, and 6.3%, respectively. The average $J(0)$ and $J(\omega_N)$ values for residues from 9 to 29, a tight turn and α-helix, were 1.4 ns/rad and 0.52 ns/rad (Table 1). These $J(0)$ and $J(\omega_N)$ values agree well with those derived by Peng and Wagner (1992a), 1.37 ns/rad (0.13 ns/rad) and 0.48 ns (0.02 ns), respectively.

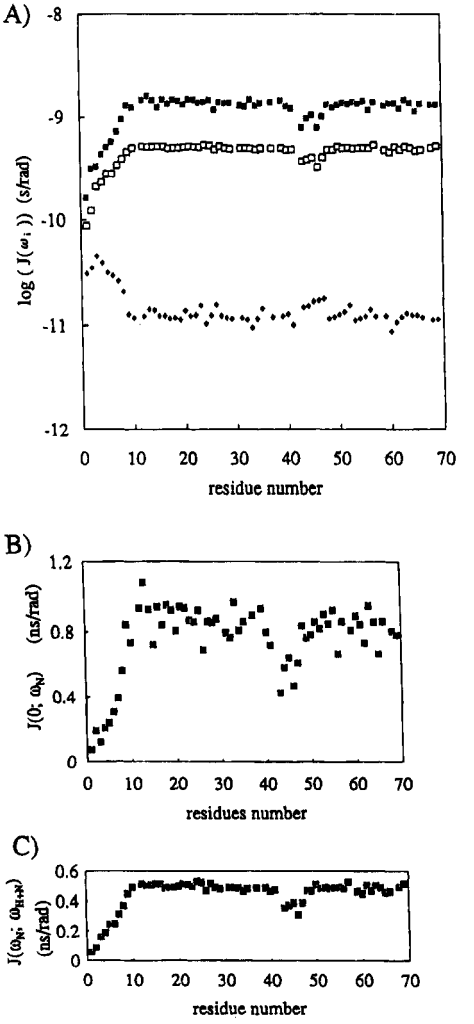

FIGURE 1: (A) $J(0)$ (■), $J(\omega_N)$ (□), and $J(\omega_H + \omega_N)$ (◆) values calculated using QSDF analysis, (B) $J(0; \omega_N)$ defined by $J(0) - J(\omega_N)$, and (C) $J(\omega_N; \omega_{H+N})$ defined by $J(\omega_N) - J(\omega_H + \omega_N)$ for eglin *c*.

No significant variation in the $J(0; \omega_N)$ is observed at residue numbers 9−40 and 49−69. Reduced values in the $J(0; \omega_N)$ and $J(\omega_N; \omega_{H+N})$ are observed at the protease binding loop (residue numbers 41−48) and at the N-terminal eight residues. This indicates that the motions faster than nanosecond in the protease binding loop are dominant compared with other regions in the protein.

The large $J(\omega_H + \omega_N)$ values at the N-terminal residues seen in Figure 1 are not visible in the spectral densities derived by Peng and Wagner (1992a). Our results for the $J(0)$, $J(\omega_N)$, and $J(\omega_H + \omega_N)$ values at the N-terminal residues lead to a reasonable picture, where the N-terminal segment is more flexible than the remaining structural part of the protein.

The QSDF Analysis of Glucose Permease IIA. The $J(0)$, $J(\omega_N)$, and $J(\omega_H + \omega_N)$ values for glucose permease IIA domain are shown in Figure 2. Intrinsic errors were estimated to be 3.8%, 3.2%, and 15%, respectively. The values of the $J(0; \omega_N)$ and the $J(\omega_N; \omega_{H+N})$ at the N-terminal residues are smaller than those at other regions. The absolute values of the $J(\omega_N; \omega_{H+N})$ at the N-terminal residues in this protein are larger than those in eglin *c* (Figure 1). Two

Table 1: Average $J(0)$, $J(\omega_N)$, and $J(\omega_H + \omega_N)$ Values for Eight Protein Systems Obtained Using the QSDF Analysis and Average $J(0)_{ls}$ Values Using the Model-Free Analysis[a]

		QSDF			model-free analysis		
		$J(0)$ (ns/rad)	$J(\omega_N)$ (ns/rad)	$J(\omega_H + \omega_N)$ (ps/rad)	$S^{2\,b}$	$\tau_R{}^b$ (ns)	$J(0)_{ls}$ (ns/rad)
eglin c[c]	av	1.4	0.52	12.6	0.83	4.2	1.4
	dev	0.07	0.012	1.1			
FK506BP free	av	4.9	0.33	6.1	0.88	9.2	3.2
	dev	1.3	0.02	1.2			
FK506BP bound	av	3.4	0.34	4.0	0.88	9.0	3.1
	dev	0.23	0.017	1.2			
ras p21	av	3.5	0.23	16.5			
	dev	0.36	0.02	0.12			
thioredoxin reduced	av	2.4	0.44	10	0.87	6.3	2.2
	dev	0.22	0.031	1.5			
thioredoxin oxidized	av	2.3	0.42	9.8	0.86	6.4	2.2
	dev	0.19	0.025	1.4			
GPIIA[d]	av	1.9	0.38	7.5	0.75−0.9	6.2	1.9−2.2
	dev	0.17	0.023	0.81			
calmodulin							
N-domain[e]	av	2.5	0.4	9.3	0.82	7.1	2.3
	dev	0.26	0.02	1.2			
C-domain[f]	av	2.1	0.41	11	0.8	6.3	2.0
	dev	0.27	0.026	1.8			

[a] The $J(0)$ for the model-free analysis were described as $J(0)_{ls}$ (Peng & Wagner, 1992a). [b] These were obtained from the literature (see text). [c] The average taken for residues from 9 to 29. [d] Glucose permease IIA domain. Residues 20−150 were used in the QSDF analysis. [e] Residues 1−70. Data obtained from the literature (Barbato et al., 1992). Preliminary analysis was reported (Ishima & Nagayama, 1995). [f] Residues 80−147.

causes are thought to be attributed to the difference of the $J(\omega_N; \omega_{H+N})$ between the two proteins. One is that the N-terminal residues of eglin c undergo faster internal motions than those of glucose permease IIA domain. The other reason is that the distribution of the spectral density function of the glucose permease IIA domain is shifted to frequencies lower than that of eglin c because the molecular mass of eglin c is about two times smaller than that of the glucose permease IIA domain.

The region from residues 21 to 58 shows small variations in the $J(0; \omega_N)$ and the $J(\omega_n; \omega_{H+N})$, for example, residues 20−22, 31−33, 40−42, and 50−52. Those are located in just the beginning of the β-strand or loop regions or between β-strands. The $J(0; \omega_N)$ varied little in the region from 59−130, which includes an active site (64−69). However, an irregular increase in the $J(0; \omega_N)$ is observed at His 66 at the active site. On the other hand, no variation in the $J(\omega_N; \omega_{H+N})$ is observed in this region. In the region from residue 130 to the C-terminus, small variations in the $J(0; \omega_N)$ and also in the $J(\omega_N; \omega_{H+N})$ values are again observed. These regions correspond to short β-strands and a loop. The relaxation data and the model-free analysis performed by Stone (1992) also indicated dynamics for the regions described above, though the model-free analysis cannot distinguish the changes in the $J(0; \omega_N)$ and the $J(\omega_N; \omega_{H+N})$.

The QSDF Analysis of FK506 Binding Protein. The $J(0)$, $J(\omega_N)$, and $J(\omega_H + \omega_N)$ values of FK506 binding protein in the free state and the FK506 bound state (Cheng et al., 1993, 1994) are shown in Figure 3. The intrinsic errors of the $J(0)$ and the $J(\omega_N)$ were estimated to be less than 5% for the majority. Large variation of the values of the $J(0; \omega_N)$ is observed in the free state. The upper bound of the $J(0; \omega_N)$ is 7.0 ns/rad, and the lower bound of the $J(0; \omega_N)$ is 3.0 ns/rad (Figure 3, left). The variation is dramatically suppressed in the bound state to a unique value of around 3.4 ns/rad (Figure 3, right). The average $J(\omega_N)$ values were 0.33 and 0.34 ns/rad for free and bound states, respectively. The values of the $J(\omega_N; \omega_{H+N})$ in the free state are almost unique except for the loop region (78−95).

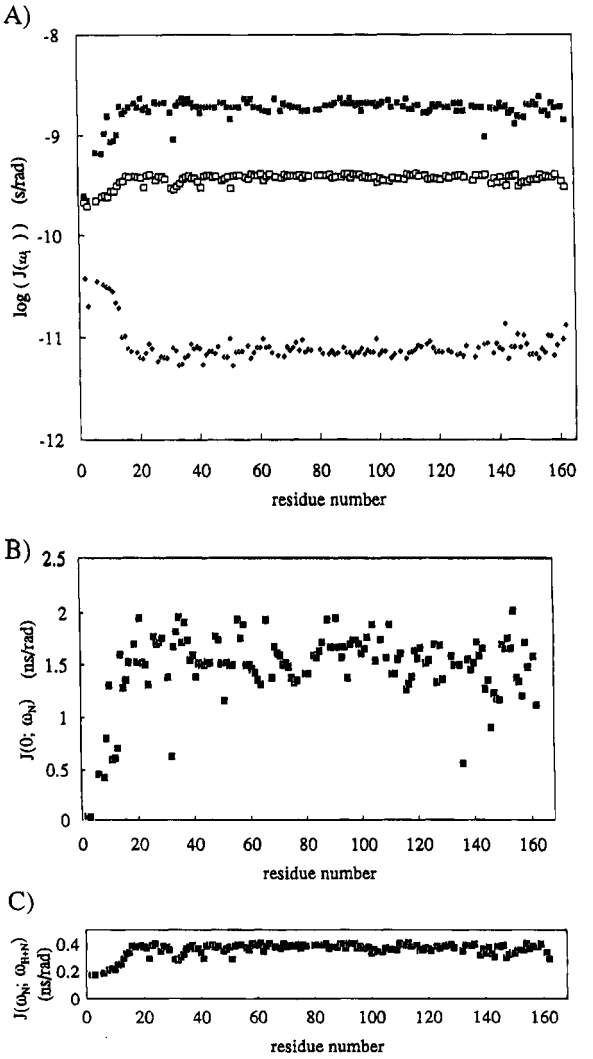

FIGURE 2: (A) $J(0)$ (■), $J(\omega_N)$ (□), and $J(\omega_H + \omega_N)$ (◆) values calculated using QSDF analysis, (B) $J(0; \omega_N)$ values, and (C) $J(\omega_N; \omega_{H+N})$ values for glucose permease IIA.

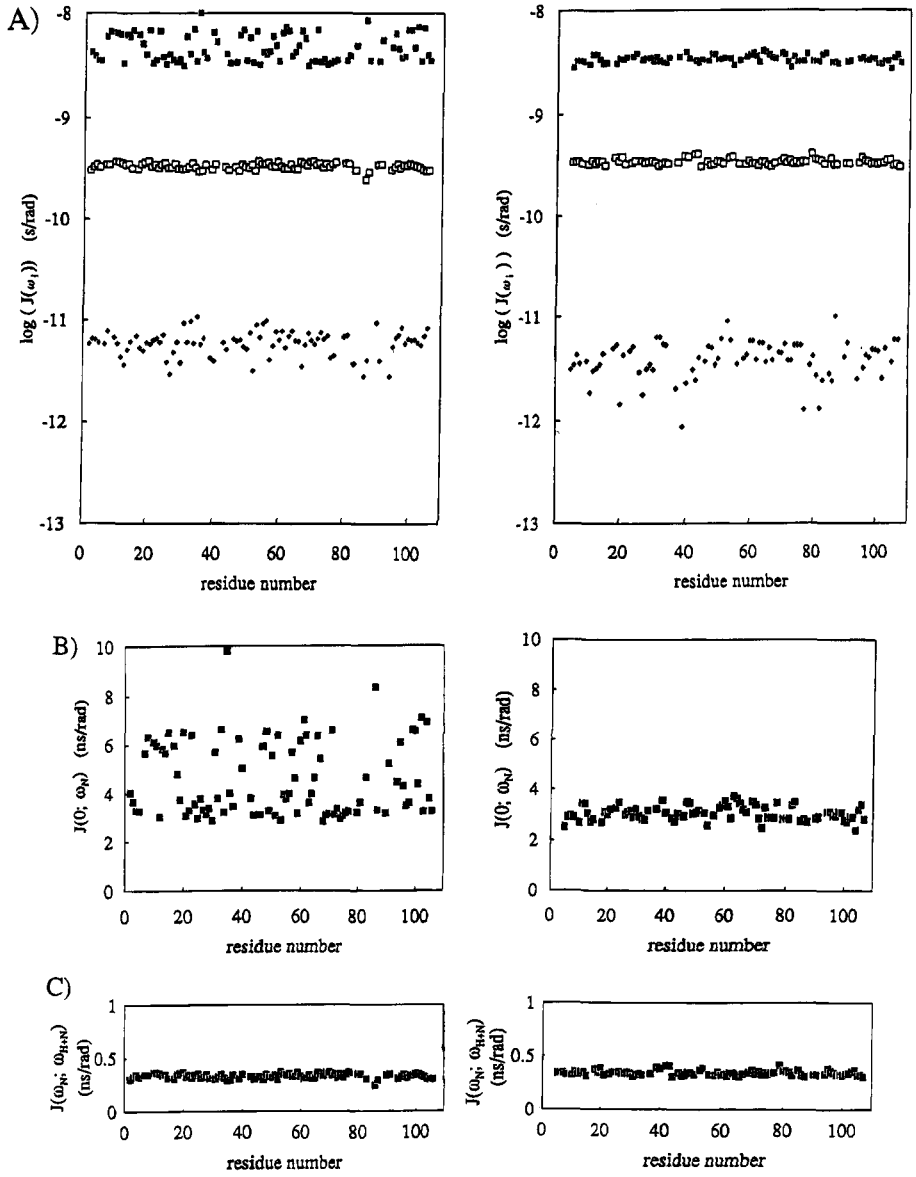

FIGURE 3: (A) $J(0)$ (■), $J(\omega_N)$ (□), and $J(\omega_H + \omega_N)$ (◆) values calculated using QSDF analysis, (B) $J(0; \omega_N)$ values, and (C) $J(\omega_N; \omega_{H+N})$ values for the free (left) and bound (right) state with FK506 of FK506 binding protein.

Now we consider whether the changes in the $J(0; \omega_N)$ values between the free and bound states are due to internal motions or to overall tumbling motions. Using the values for $J(0; \omega_N)$, we can focus on only motions slower than ω_N^{-1}. Then, these values reveal two possibilities. (i) The molecular tumbling mainly contributes to the $J(0; \omega_N)$ value of 7 ns/rad for the free state and contributes to that of 3 ns/rad for the bond state. (ii) The molecular tumbling contributes to the $J(0; \omega_N)$ value of 3 ns/rad for both states. Because the molecular mass of the protein is 11 000 and 12 000 in the free and bound states, we estimate the correlation time of the molecular tumbling to be above 3 ns, which is close to ω_N^{-1}. In this respect, both cases i and ii are valid. For case i, the $J(\omega_N)$ values between the free and bound states should differ because the change in molecular tumbling influences the effective τ_i, according to eq 14. Because no significant differences in the $J(\omega_N)$ occurred between the free and bound states (Table 1), case ii seems more reasonable. We tentatively conclude that the large values for the $J(0; \omega_N)$ in the free state arise from internal motions characteristic to this protein and that these values diminish after the FK506 binds to the protein (Figure 4). The slight changes in the $J(\omega_N)$ values between the two states seem to stem from the small difference in the molecular weights between the two states.

Reduced values of $J(\omega_N; \omega_{H+N})$ in the loop region including 86 and 87 residues are observed in the free state. On the other hand, the value of the $J(0; \omega_N)$ at the 86 residue is large. The motion of the loop has been shown using the model-free analysis by Cheng et al. (1994). The dramatic change in the $J(0; \omega_N)$ when FK506 becomes bound to the protein has been interpreted by Cheng et al. (1994) as an exchange in conformation, which induces a change in chemical shift. However, they concluded that the molecular tumbling of the free state was larger than that of the bound state, which is completely opposite to our analysis.

The QSDF Analysis of Thioredoxin. The $J(0)$, $J(\omega_N)$, and $J(\omega_H + \omega_N)$ values are shown in Figure 5 for the oxidized and reduced states of thioredoxin. Intrinsic errors for $J(0)$, $J(\omega_N)$, and $J(\omega_H + \omega_N)$ were 1.3%, 2.5%, and 3.6% for the oxidized state and 1.8%, 1.3%, and 2.9% for the reduced state, respectively. The average $J(0)$ and $J(\omega_N)$ values in the oxidized state are slightly larger than those in the reduced state.

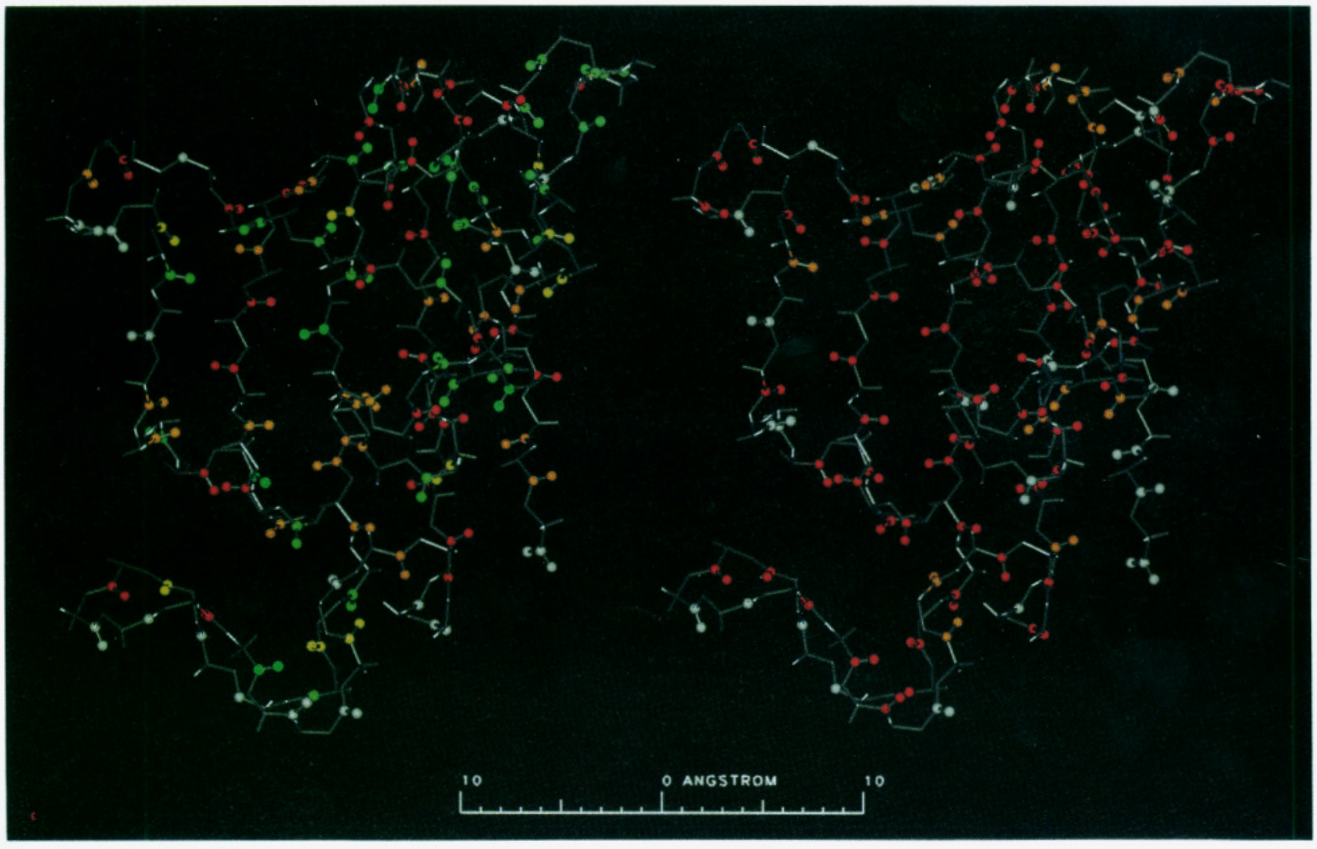

FIGURE 4: Mapping of $J(0; \omega_N)$ values of amide N-15 nuclei in FK506 binding protein in the free state (left) and bound state (right) with FK506. Both protein structures were generated from the crystal structure of the bound state, 1FKF, in the Protein Data Bank, and displayed using the MolSkop system (JEOL Ltd., Japan). The values of the $J(0; \omega_N)$ from large to small were represented by green, yellow, orange, and red. The attached protons to the amide N-15 nuclei were also colored.

Thioredoxin in the oxidized state has a disulfide bond between Cys 32 and Cys 35 at the active site. This disulfate bond is broken in the reduced state, leading to disulfide reductase activities (Holmgren, 1985). As seen in Figure 5, the values for the $J(0; \omega_N)$ at residues 32, 33, 73−75, and 85 are higher for the reduced state than for the oxidized state. On the other hand, the $J(\omega_N; \omega_{H+N})$ values decreased at residues 28 and 33 in the reduced state. We interpret these trends in the values of $J(0; \omega_N)$ and $J(\omega_N; \omega_{H+N})$ as increases in the motion slower than ω_N^{-1} near the active site.

Residues from 73 to 75 are located near the active site. The $J(0; \omega_N)$ values at residues 73, 74, and 75 show the variation of 73 (small) − 74 (very small) − 75 (middle) in the oxidized state and of 73 (large) − 74 (small) − 75 (very large) in the reduced state. [The words in parentheses indicate relative values of the $J(0; \omega_N)$.] This suggests a correlated change in the internal motion among regions due to the redox reaction. Residues from 91 to 94 also are located near the active site. In this case, the $J(0; \omega_N)$ at residues 91, 92, 93, and 94 decreased monotonically for both states. The absolute $J(0; \omega_N)$ for residue 91 increases in the reduced state. In the reduced state, residue 85 shows an increase in the $J(0; \omega_N)$ and residue 86 shows a slight decrease in the $J(\omega_N; \omega_{H+N})$. Although residue 85 and 86 are located opposite the active site, these residues undergo changes in dynamics after the reduction. These residues are connected to residues 91−94 through one β-sheet. It is shown here that the change of internal motions at the active site propagates to the side opposite the proteins through one β-sheet (Figure 6).

The QSDF Analysis of ras p21 Protein. Figure 7 shows the $J(0)$, $J(\omega_N)$, and $J(\omega_H + \omega_N)$ values of ras p21 protein in its GDP form (Kraulis et al., 1994; residues 1−166). The average $J(\omega_N)$ value of ras p21, which was obtained at 600 MHz (Kraulis et al., 1994), is smaller than those obtained at 500 MHz for other proteins shown in this paper (Table 1).

Reduced values for the $J(0; \omega_N)$ are observed at the N- and C-terminal residues compared with other residues, but the values are not as large as those observed in eglin *c* or the glucose permease IIA domain. Moreover, reduced values for the $J(\omega_N; \omega_{H+N})$ are not observed at the C-terminal residues. These indicate that the terminal regions are not so flexible. These trends agree well with the fact that both the N-terminus and C-terminus of this protein consist of secondary structures as pointed out by Kraulis et al. (1994) in their analysis. At residues 26−32 and 56−70, the values for the $J(0; \omega_N)$ are smaller than the average values. At residues 35−37, they are larger than the average values. No reduction in $J(\omega_N; \omega_{H+N})$ is observed in these regions. Therefore, motions slower than nanosecond are slightly decreased in these regions. These regions correspond to loop 2 and loop 4, respectively, where the protease interacts with GDP or GTP (Kraulis et al., 1994; Milburn et al., 1990). The regions at residues 105−109 and 122−124 are located near the guanine base. In these regions, not only the $J(0; \omega_N)$ but also the $J(\omega_N; \omega_{H+N})$ values are reduced. Kraulis et al. (1994) analyzed relaxation data using a T_1/T_2 ratio and compared that with NOE data. Because the T_1/T_2 ratio fairly represents the ratio of $J(0)$ to $J(\omega_N)$, their interpretation of

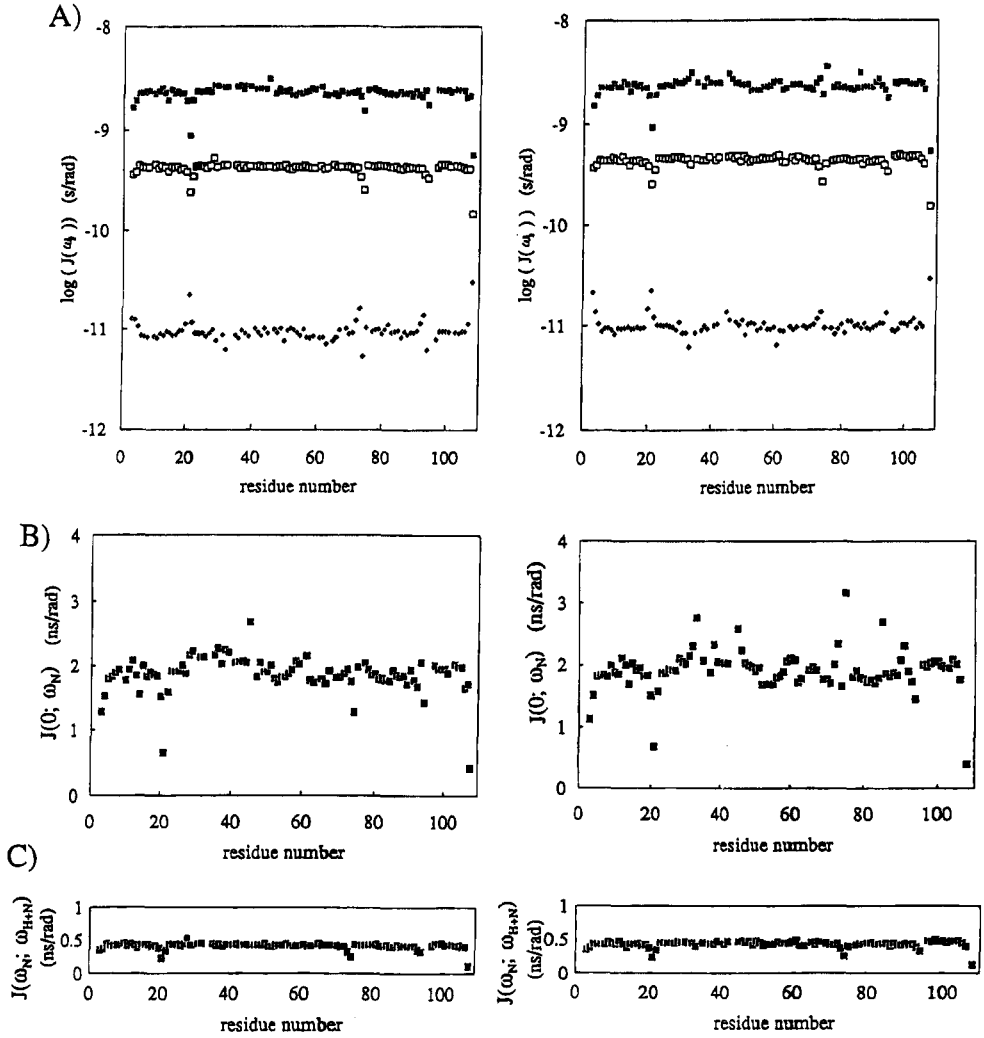

FIGURE 5: (A) $J(0)$ (■), $J(\omega_N)$ (□), and $J(\omega_H + \omega_N)$ (◆) values calculated using QSDF analysis, (B) $J(0; \omega_N)$ values, and (C) $J(\omega_N; \omega_{H+N})$ values for thioredoxin in its oxidized (left) and reduced (right) states.

the protein dynamics agrees well with our results from the QSDF analysis.

The $J(0; \omega_N)$, the $J(\omega_N; \omega_{H+N})$, and the QSDF Analysis. Using the QSDF analysis, we obtained the $J(0)$, $J(\omega_N)$, and $J(\omega_H + \omega_N)$ values for amide N-15 nuclei in eight protein systems in Table 1. The experimental values we used were almost within the range of theoretical NOE values when no resonant motions were present, i.e., −3.6 to 0.82 at 500-MHz NMR (Kay et al., 1989). If a significant amount of resonant motion exists, the NOE values should exceed 0.82 at $\omega^2\tau^2 \gg 1$ (Ishima & Nagayama, 1995). Only when the resonant motion exists just at the resonance frequency with considerable intensity does it affect the spectral density. Recent molecular dynamics simulations revealed time correlations of N−H vectors (Balasubramanian et al., 1994; Eriksson et al., 1993). These indicated that such resonant motions only appear coupled with dissipative internal motions. This drastically reduces the contribution of resonant motion to the apparent intensity of the spectral density. Therefore, the assumption of eq 5 must be valid in the studies shown here (Ishima & Nagayama, 1995).

Most $J(0)$ values are 5−10 times larger than the $J(\omega_N)$ values, which are again about 10 times larger than the $J(\omega_H + \omega_N)$ values as described in Table 1. Considering these orders of magnitude, the RN (eq 8) is almost determined by the $J(\omega_H + \omega_N)$, the T_1^{-1} (eq 6) by the $J(\omega_N)$, and the T_2^{-1} by the $J(0)$ (eq 7). Therefore, quantitative evaluation of T_1 and T_2 values themselves gives information analogous to the spectral densities by assuming $J(0) \gg J(\omega_N) \gg J(\omega_H + \omega_N)$.

A framework that can be used to interpret spectral densities with effective motions has long been needed. For the purpose, we adopted the $J(0; \omega_N)$ and the $J(\omega_n; \omega_{H+N})$. The meaning of $J(0; \omega_N)$ and $J(\omega_N; \omega_{H+N})$ is particularly important because those values originated from the motions slower than ω_N^{-1} and $(\omega_H + \omega_N)^{-1}$ are focused on. We now discuss two points to clarify the meaning of the $J(0; \omega_N)$ and $J(\omega_N; \omega_{H+N})$. The first point is that the word "motion", for example that used in "motions slower than ω_{H+N}^{-1}", does not describe motions given by a physical motional process. If a physical motional process is anisotropic, then it can be represented by the plural terms in eq 11, and therefore, the sum of the terms that have longer correlation times does not necessarily correspond to individual physical motional processes (Lipari & Szabo, 1982a). The second point is that a_i and τ_i are combined in the function and, thus, inseparably contribute to the $J(0; \omega_N)$ and $J(\omega_N; \omega_{H+N})$. The a_i and τ_i can only be separated as the relaxation spectrum by theoretical approach based on a concrete motional model (Fujiwara & Nagayama, 1985). Although, it is very difficult to estimate all terms in eq 11, we should not adopt the approximation of eq 11 with a small number of a_i and τ_i values. Otherwise, details of the slower motions, which are our interest, become

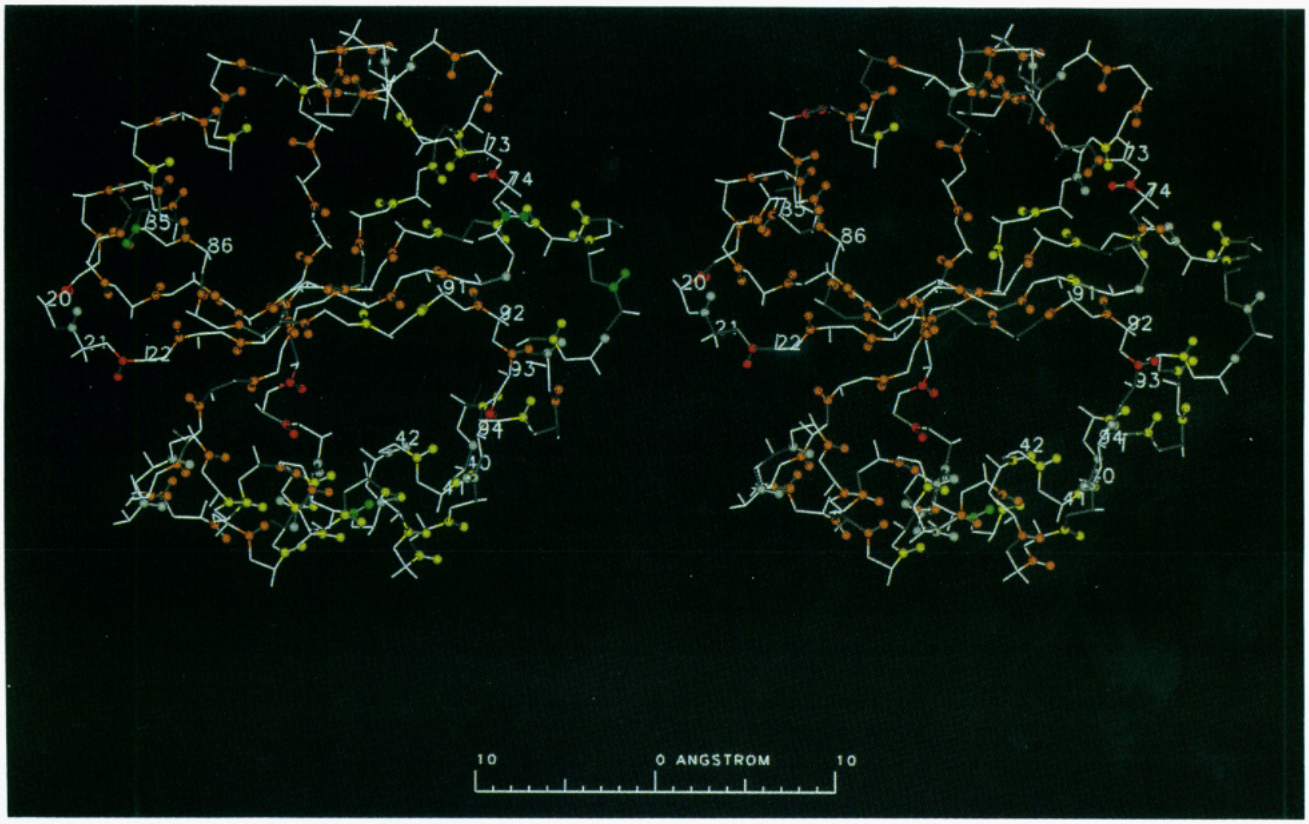

FIGURE 6: Mapping of $J(0; \omega_N)$ values of amide N-15 nuclei in thioredoxin in the oxidized (left) and reduced (right) state. Both protein structures were generated from the first structure of 1TRX in the Protein Data Bank and were displayed using the MolSkop system (JEOL Ltd., Japan). The values for $J(0; \omega_N)$ from large to small were represented by green, yellow, orange, and red. The attached protons to the amide N-15 nuclei were also colored.

obscured. Therefore, we directly used the $J(0; \omega_N)$ and $J(\omega_N; \omega_{H+N})$ to discuss the terms with longer τ_i than the ω_N^{-1}.

Comparison of the QSDF Analysis with Other Analysis Techniques. We compared the values of $J(0)$, $J(\omega_N)$, and $J(\omega_H + \omega_N)$ calculated by Peng and Wagner (1992) with those obtained using the QSDF analysis. In the core region of eglin *c*, the $J(0)$, $J(\omega_N)$, and $J(\omega_H + \omega_N)$ values obtained using the two methods agree well with each other. On the other hand, more reasonable $J(\omega_H + \omega_N)$ values at the N-terminal residues (Figure 1) were observed in the QSDF analysis than in the analysis of Peng and Wagner (1992a). High-frequency internal motions of the N-terminal residues are obvious not only from the QSDF analysis but also from the model-free analysis, or from evaluating the NOE values. Peng and Wagner pointed out large errors crucial in the spectral densities of high frequencies. We can understand the error arising from the relaxation rate of N-15 antiphase relaxation rates, which explicitly include the longitudinal magnetization of the coupled proton and which are sensitively influenced by strong spin diffusion and chemical exchange of the proton spin. If these relaxation rates are precisely evaluated by proper correction, the spectral densities would agree with those we obtained using the QSDF analysis. However, the method of Peng and Wagner (1992b) itself is very important to pursuit distribution of spectral densities for a system in which eq 5 cannot be assumed, such as for a system of C-13 nuclei.

Compared with the model-free analysis, the benefit of the QSDF analysis is that the motions slower than nanosecond can be evaluated without any bias by using the $J(0; \omega_N)$ and the $J(\omega_N; \omega_{H+N})$. In the model-free analysis, quantitative evaluation of the slow internal motion that is on the same time scale as molecular tumbling is difficult because internal motions and molecular tumbling have to be separated into two distinct motional processes. The enormous number of terms in eq 15 cannot be safely approximated by only two terms. In the model-free analysis, the slow motional processes are separately evaluated as an additional relaxation time, R_{ex}, to the transverse relaxation time (Stone et al., 1990). After the removal of the R_{ex} term, the order parameter and the effective correlation time are calculated. This reveals the major reason for the average $J(0)$ values obtained by the QSDF analysis being larger than those obtained by the model-free analysis, the $J(0)_{ls}$, where the slow motional process was removed (Table 1). Even if such an evaluation of the slow internal motion is performed in the model-free analysis (Palmer et al., 1992; Stone et al., 1993), the analysis cannot accurately characterize a protein when the slower internal motions in a protein are large, because the rotational correlation time of the protein is estimated with a bias to the slower one. It was seen in FK506 protein. The R_{ex} term is given as the difference between the experimental T_2^{-1} value and the model one. The R_{ex} term, therefore, will not be free from remainders of $J(0)$ components unconsidered in the model as well as the exchange term. It is difficult to evaluate the exchange term without accounting for the entire aspect of protein dynamics. Our QSDF analysis opens a way to evaluate the entire aspect of the protein internal motions.

Biological Findings for the Investigated Proteins. Significance of the QSDF analysis is easily appreciated by new findings in protein dynamics. One significant feature of the

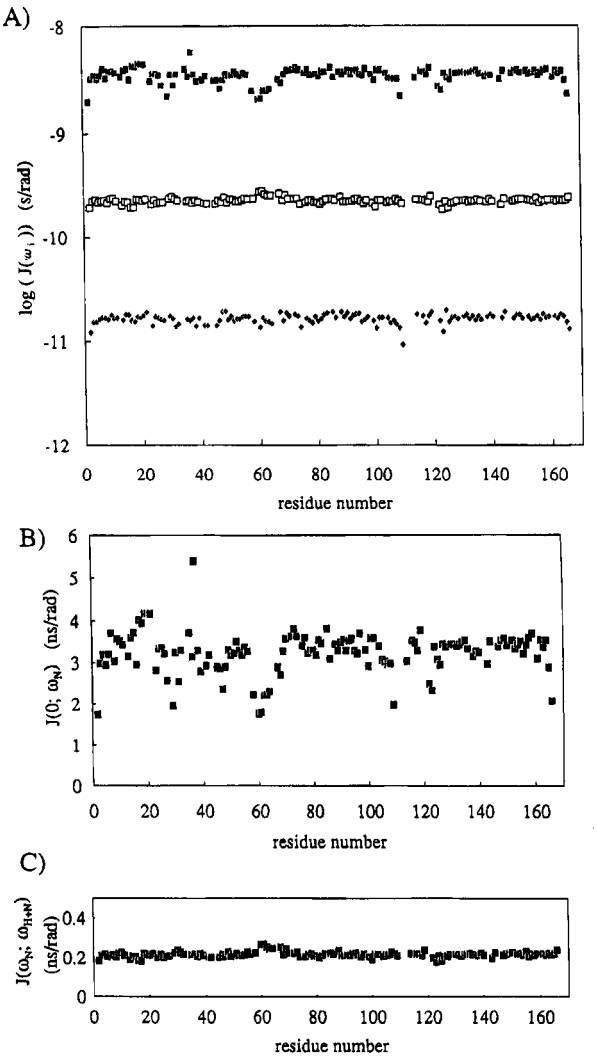

FIGURE 7: (A) $J(0)$ (■), $J(\omega_N)$ (□), and $J(\omega_H + \omega_N)$ (◆) values calculated using QSDF analysis, (B) $J(0; \omega_N)$ values, and (C) $J(\omega_N; \omega_{H+N})$ values for ras p21-GDP.

QSDF analysis is that the $J(0; \omega_N)$ is sensitive to the change in dynamics at biologically relevant sites such as at active sites. We showed that the active site of eglin *c* has a motional behavior different from those observed at the flexible terminal regions. The FK506 binding protein showed large changes in the $J(0; \omega_N)$. Internal motions at individual residues could be discussed in detail for ras p21-GDP and thioredoxin by referring to the $J(0; \omega_N)$. In thioredoxin, changes in internal motions were observed not only around the active site but also at the site opposite the protein, which is connected to the active site through one β-sheet. Although there are several analyses to extract low-frequency internal motions (Peng et al., 1992; Szyperski et al., 1993; Brüschweiler, 1992), the QSDF analysis is fairly successful in extracting a wider range of motional processes.

The second significant feature is that correlation of motions can be discussed from the local changes in the $J(0)$ and the $J(\omega_N)$ values. In calmodulin (Ishima & Nagayama, 1995), a set of three neighboring residues showed correlation in the $J(0)$ and the $J(\omega_N)$ values. In our study, we observed correlations in the changes of spectral density values at residues 73−to 75 in thioredoxin. Although this tendency was observed in other proteins, these were within the error ranges. This local correlation suggests that there is a portion of small hinge composed of two or three residues characterizing the spectral density function as such. The hinge usually is located between two secondary structures, and hence independent fluctuations of two secondary structural units are restricted to some extent.

ACKNOWLEDGMENT

We thank Dr. Endo for his help in the graphic presentation of protein structures and Dr. Yang for his insightful discussion.

REFERENCES

Balasubramanian, S., Nirmala, R., Beveridge, D. L., & Bolton, P. H. (1994) *J. Magn. Reson., Ser. B 104*, 240−249.
Barbato, G., Ikura, M., Kay, L. E., Pastor, R. W., & Bax, A. (1992) *Biochemistry 31*, 5269−5278.
Bax, A., Griffey, R. H., & Hawkins, B. L. (1983) *J. Magn. Reson. 55*, 301−315.
Brüschweiler, R. (1992) *J. Am. Chem. Soc. 114*, 5341−5344.
Cheng, J. W., Lepre, C. A., Chambers, S. P., Fulghum, J. R., Thomson, A. J., & Moore, J. M. (1993) *Biochemistry 32*, 9000−9010.
Cheng, J. W., Lepre, C. A., & Moore, J. M. (1994) *Biochemistry 33*, 4093−4100.
Clore, G. M., Driscoll, P. C., Wingfield, P. T., & Gronenborn, A. M. (1990) *Biochemistry 29*, 7387−7401.
Eriksson, M. A. L., Berglund, H., Härd, T., & Nilsson, L. (1993) *Proteins 17*, 375−390.
Fujiwara, T., & Nagayama, K. (1985) *J. Chem. Phys. 83*, 3110−3117.
Goldman, M. (1984) *J. Magn. Reson. 60*, 437−452.
Griffry, R. H., Redfield, A. G., Loomis, R. E., & Dahlquist, F. W. (1985) *Biochemistry 24*, 817−822.
Holmgren, A. (1985) *Annu. Rev. Biochem. 54*, 237−271.
Ishima, R., & Nagayama, K. (1995) *J. Magn. Reson.* (in press).
Ishima, R., Shibata, S., & Akasaka, K. (1991) *J. Magn. Reson. 91*, 455−465.
Kay, L. E., Torchia, D. A., & Bax, A. (1989) *Biochemistry 28*, 8972−8979.
Kay, L. E., Nicholson, L. K., Delaglio, F., Bax, A., & Torchia, D. A. (1992) *J. Magn. Reson. 97*, 359−375.
King, R., & Jardetzky, O. (1978) *Chem. Phys. Lett. 55*, 15−17.
Kraulis, P. J., Domaille, P. J., Campbell-Burk, S. L., Aken, T. V., & Laue, E. D. (1994) *Biochemistry 33*, 3515−3531.
Lipari, G., & Szabo, A. (1982a) *J. Am. Chem. Soc. 104*, 4546−4559.
Lipari, G., & Szabo, A. (1982b) *J. Am. Chem. Soc. 104*, 4559−4570.
Milburn, M. V., Tong, L., deVos, A. M., Brünger, A., Yamaizumi, Z., Nishimura, S., & Kim, S.-H. (1990) *Science 247*, 939−945.
Nirmala, N. R., & Wagner, G. (1988) *J. Am. Chem. Soc. 110*, 7557−7559.
Palmer, A. G., III, & Case, D. A. (1992) *J. Am. Chem. Soc. 114*, 9059−9067.
Peng, J. W., & Wagner, G. (1992a) *Biochemistry 31*, 8571−8586.
Peng, J. W., & Wagner, G. (1992b) *J. Magn. Reson. 98*, 308−332.
Peng, J. W., Thanabal, V., & Wagner, G. (1991) *J. Magn. Reson. 94*, 82−100.
Ribeiro, A. A., King, R., Restivo, C., & Jardetzky, O. (1980) *J. Am. Chem. Soc. 102*, 4040−4051.
Slicter, C. P. (1978) *Principles of Magnetic Resonance*, Springer-Verlag, New York.
Stone, M. J., Fairbrother, W. J., Palmer, A. G., III, Reizse, J., Saier, M. H., Jr., & Wright, P. E. (1992) *Biochemistry 31*, 4394−4406.
Stone, M. J., Chandrasekhar, K., Holmgren, A., Wright, P. E., & Dyson, H. J. (1993) *Biochemistry 32*, 426−435.
Szyperski, T., Luginbuehl, P., Otting, G., Guentert, P., & Wüthrich, K. (1993) *J. Biomol. NMR 3*, 151−164.
Wagner, G. (1993) *Curr. Opin. Struct. Biol. 3*, 748−754.

BI9418939